Algebraic Quantum LDPC Codes for Low-Overhead, Single-Shot Fault Tolerance

Research Overview

Feroz Ahmed Mian

Manning College of Information and Computer Sciences, University of Massachusetts Amherst

Advisor: Prof. Stefan Krastanov · fmian@umass.edu · fe-r-oz.github.io · github.com/Fe-r-oz

Abstract

My research asks how to build quantum error-correcting codes that are *simultaneously* high-rate, high-distance, low-weight, and cheap to decode, and how to verify these properties numerically at sizes that matter for real hardware. I work at the meeting point of commutative algebra, expander-graph combinatorics, and circuit-level simulation. This overview covers two first-author projects and the open-source software behind them. (i) *Multivariate multicycle (MM) codes* [1] give a Koszul-complex description of abelian multicycle codes. The description covers bivariate bicycle, multivariate bicycle, abelian two-block group algebra, generalized bicycle, trivariate tricycle and toric codes. It supplies closed-form parity-check and, for $t \geq 4$, metacheck matrices for both sectors, which make large searches and single-shot decoding experiments straightforward. (ii) *Quantum Tanner (QT) codes at moderate blocklength* [2] answers an open question from Ref. [3] with a search over non-abelian groups that finds instances with $n \in [500, 1000]$ and distance upper bounds above 20, benchmarked under phenomenological and circuit-level noise. Both projects rest on code infrastructure I lead in `QuantumClifford.jl`, `QECCore.jl`, and `QuantumExpanders.jl`. I close with open directions relevant to reconfigurable neutral-atom hardware.

1 Motivation

Two-dimensional local codes such as the surface code obey the Bravyi–Poulin–Terhal bound $kd^2 \leq cn$ [4], so every extra logical qubit costs a full patch of physical qubits. Quantum LDPC codes escape this trade-off by giving up geometric locality while keeping checks sparse. Bivariate bicycle codes [5] showed that the escape can already pay off at around a hundred qubits. Reconfigurable atom arrays are a natural home for such codes: parallel atom rearrangement with crossed acousto-optic deflectors can implement the non-local syndrome-extraction circuits of product-structured qLDPC codes with low overhead [6].

Memory parameters $[[n, k, d]]$ are only part of the story. A practical code must also (a) tolerate noisy syndrome measurements without $\mathcal{O}(d)$ repeated rounds; this is *single-shot* decoding [7–9]. It must (b) keep check weights low enough for shallow circuits, and (c) come with a decoder that performs well under circuit-level noise. My work targets all three.

2 Multivariate Multicycle Codes for Complete Single-Shot Decoding

Construction. Fix the ideal $I = \langle x_1^{\ell_1} - 1, \ldots, x_D^{\ell_D} - 1 \rangle$, so that $S = \mathbb{F}_2[x_1, \ldots, x_D]/I \cong \mathbb{F}_2[\mathbb{Z}_{\ell_1} \times \cdots \times \mathbb{Z}_{\ell_D}]$. Choose t elements $F_1, \ldots, F_t \in S$ and form the Koszul complex $K_\bullet(F_1, \ldots, F_t; S)$, whose degree-$k$ term is free of rank $\binom{t}{k}$. This complex is an iterated lifted product of t two-term complexes, each given by a 1×1 matrix over the group algebra. MM codes are therefore a Koszul-complex formulation of the abelian multicycle (AMC) codes of Ref. [10]. For $t = 2q \geq 4$, the middle five terms

$$K_{q-2} \xleftarrow{M_X} K_{q-1} \xleftarrow{P_X} K_q \xleftarrow{P_Z^\top} K_{q+1} \xleftarrow{M_Z^\top} K_{q+2}$$

Family	$[[n, k, (d_X, d_Z)]]$	k/n	max check wt.	Observed profile ($w = 1, 2, \dots$)
4D toric [11]	$[[96, 6, (4, 4)]]$	0.06	6	4, 4, 4
Bivariate bicycle [5]	$[[144, 12, (12, 12)]]$	0.08	6	3, 4, 3, 4, 3, 4
Trivariate tricycle [12]	$[[72, 6, (12, 6)]]$	0.08	9 / 6	3, 2, 3, 2, 3, 2
Abelian multicycle [10]	$[[96, 6, (8, 8)]]$	0.06	6	4, 6, 6, 6, 4, 4
MM	$[[96, 12, (8, 8)]]$	0.12	16	8, 8, 8, 8, 8, 8
MM	$[[96, 44, (4, 4)]]$	0.45	12	8, 8, 8
MM	$[[486, 24, (12, 12)]]$	0.04	9	6, 10, 12, 14, 18, 18
MM	$[[486, 66, (9, 9)]]$	0.13	12	8, 12, 12, 16, 16, 12

Table 1: Excerpt of the observed confinement profiles in Ref. [1] (Z errors for the comparison codes; entrywise minimum over both sectors for MM codes). Entries are the smallest nonzero syndrome weight found by a connected-cluster search with `dist-m4ri` [13]. They describe the visited clusters, not certified minima.

define a balanced *metacheck CSS code*. Qubits live on K_q, the inner maps are the X and Z checks, and the outer maps are metachecks (checks on checks) for *both* sectors. The practical advantage is that the exterior algebra gives these matrices in closed form for every t. In the paper we also determine when an MM code encodes logical qubits, count the check relations that metachecks do not generate, and show that for even t the X and Z sectors are equivalent up to permutations.

Codes. A numerical search over the explicit check matrices gives codes with certified parameters including $[[96, 12, 8]]$, $[[144, 12, 12]]$, $[[486, 24, 12]]$, $[[630, 70, 9]]$ and $[[648, 60, 9]]$ [1]. We also give examples with five to nine Koszul generators over a single cyclic group, with check weights between 6 and 12. Table 1 lists observed confinement profiles: for each error weight, the smallest nonzero syndrome weight found among the irreducible errors visited by a connected-cluster search. These profiles are finite-size diagnostics rather than certified bounds, but small errors in the MM codes visibly produce larger syndromes than in the comparison codes.

Decoding experiments. I built Stim [14] memory circuits and decoded them with Tesseract [15], BP+OSD [16], and an overlapping-window decoder (OWD) [17]. Under phenomenological noise, adding the metacheck rows improves the single-stage decoder for the MM $[[144, 12, 12]]$ code (Fig. 1). In *plateau experiments*, the per-round logical error rate is measured as a function of the decoding window w. There the OWD reaches low logical error rates with small windows under both phenomenological and circuit-level noise (Fig. 2). I also evaluated left–right syndrome-extraction schedules [18], which avoid harmful hook errors, for weight-6 MM codes. An important open question is whether these finite-size observations extend to an asymptotic family, through soundness or confinement bounds with uniform constants.

3 Quantum Tanner Codes at Moderate Blocklength

Question. Quantum Tanner codes [19] place classical Tanner codes on the two graphs underlying a left–right Cayley complex (LRCC), and they are asymptotically good. Recent small instances, such as the weight-9 $[[144, 12, 11]]$ code, compete with the bivariate bicycle $[[144, 12, 12]]$ code [3]. That work left open whether competitive QT codes exist in the moderate regime $n \in [500, 1000]$. There is no closed formula for the rate or distance of a general lift, so the answer has to come from a well-designed search.

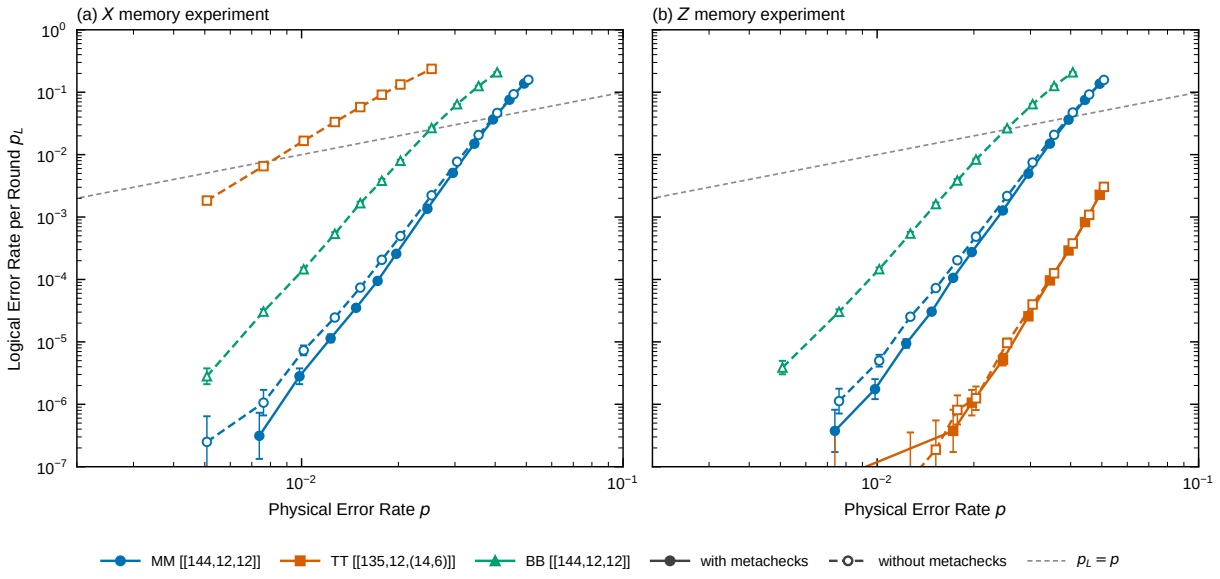


Figure 1: Single-shot decoding with metachecks under phenomenological noise: logical error rate per round after $N = 8$ noisy rounds, each decoded on its own with single-stage BP+OSD. Solid lines include the metacheck rows; dashed lines omit them. The Koszul maps supply metachecks for both check types of the MM $[[144, 12, (12, 12)]]$ code, only for the checks in (b) for the trivariate tricycle code, and for neither for the bivariate bicycle code. Figure from Ref. [1].

	Phenomenological		Circuit-level	
Code	X	Z	X	Z
$[[588, 14, (\leq 20, \leq 18)]]$	4.17%	4.62%	0.19%	0.26%
$[[648, 10, (\leq 18, \leq 20)]]$	4.28%	4.28%	0.27%	0.27%
$[[720, 6, (\leq 30, \leq 30)]]$	3.99%	4.48%	0.24%	0.24%
$[[864, 8, (\leq 39, \leq 31)]]$	3.58%	3.57%	0.14%	0.13%

Table 2: Pseudo-thresholds of four QT codes with the Tesseract decoder, defined by the crossing $p_L(p) = kp$ (phenomenological) or $p_L(p) = Tkp/10$ (circuit-level) [2].

Approach. I searched non-abelian groups from GAP's `SmallGrp` library [20] using two complementary constructions: the LRCC itself (Fig. 3) and the "lifting" view, in which a small seed CSS code is lifted by commuting left and right regular actions of $\mathcal{G}$ [3]. Candidates were pre-filtered by the distance of the associated classical Tanner codes. Distances of survivors were then bounded with two independent randomized estimators, `QDistRnd` [21] and the GPU-based `sQetch` [22], using up to 3.5×10^8 trials.

Results. The search answers the open question affirmatively. New instances include $[[480, 8, (\leq 21, \leq 21)]]$, $[[504, 4, (\leq 36, \leq 27)]]$, $[[672, 4, (\leq 48, \leq 28)]]$, $[[720, 6, (\leq 30, \leq 30)]]$, and $[[864, 8, (\leq 39, \leq 31)]]$, with check weights from 9 to 20. Seven of the eight codes highlighted in the paper's $\sqrt{n}$-barrier table satisfy $d_{\min} > \sqrt{n}$ (Fig. 4). The classical $[8, 4, 4]$ local code turned out to be a particularly good building block in this regime. All reported distances are upper bounds from randomized estimators.

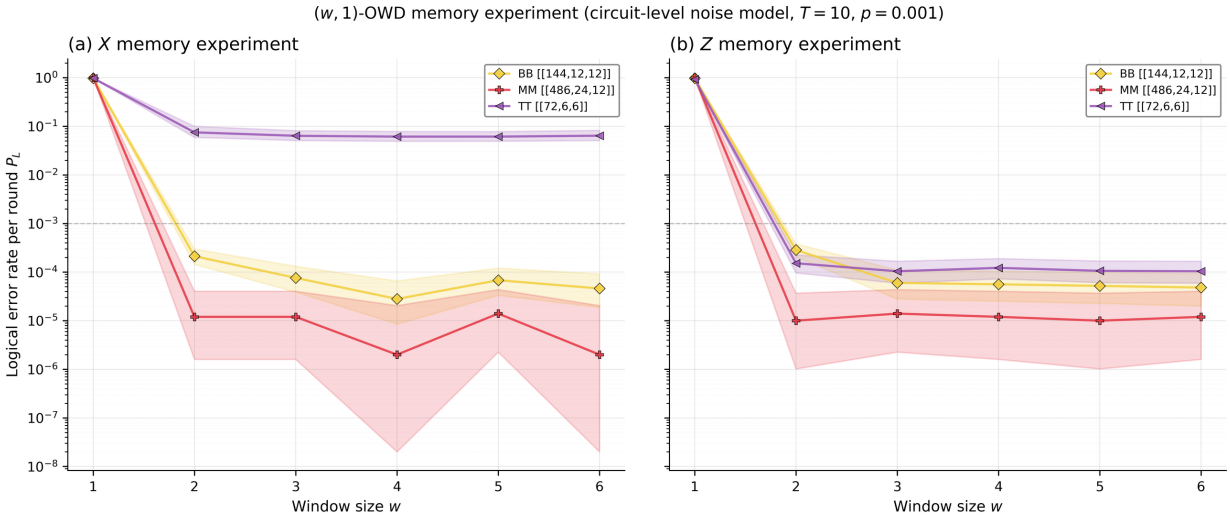


Figure 2: Few-shot plateau experiment under circuit-level noise ($T = 10$ rounds, $p = 10^{-3}$, commit $c = 1$), decoded with a $(w, 1)$ overlapping-window decoder. It compares the MM $[[486, 24, 12]]$ code with the bivariate bicycle $[[144, 12, 12]]$ and trivariate tricycle $[[72, 6, 6]]$ codes. Figure from Ref. [1].

Noise simulations. I ran X- and Z-basis memory experiments for four representative codes under phenomenological noise and under circuit-level noise. In the circuit-level model, gates, resets, and measurements fail at rate p and idle locations at $p/10$. The codes have pseudo-thresholds of 3.6–4.6% and 0.14–0.27% respectively (Table 2 and Fig. 5), in line with prior results at shorter lengths. In an appendix I compare Tesseract with the `Frontier` decoder [24] on a $[[432, 16, (\leq 15, \leq 15)]]$ code: an untuned `Frontier` raises the phenomenological pseudo-threshold from about 4.5% to 6.0%. This suggests that decoders tailored to QT structure still have substantial headroom.

4 Open-Source Infrastructure

Reproducibility is a design goal in my work. Every code reported above can be constructed with a few lines of Julia.

- **`QuantumClifford.jl` / `QECCore.jl`** [25]: I am the lead contributor of the error-correcting-code zoo. It includes MM, generalized toric, D-dimensional surface and toric codes (via `Oscar` chain complexes [26]), non-abelian lifted product, two-block group algebra codes over finitely presented groups, tile codes, and a Tillich–Zémor code variant [27].
- **Exact distances by mixed-integer programming**: a solver-agnostic `JuMP` extension (HiGHS, Gurobi, SCIP) that computes certified minimum distances of QLDPC codes. It complements the randomized estimators used for larger codes.
- **`QuantumExpanders.jl`**: LRCC and lifted constructions of QT codes, the search heuristics of Ref. [2], and explicit Morgenstern Ramanujan-graph families.
- **Simulation pipeline**: Stim/Sinter circuits [14], Tesseract, BP+OSD, and overlapping-window decoders, deployed at scale on the university HPC cluster.

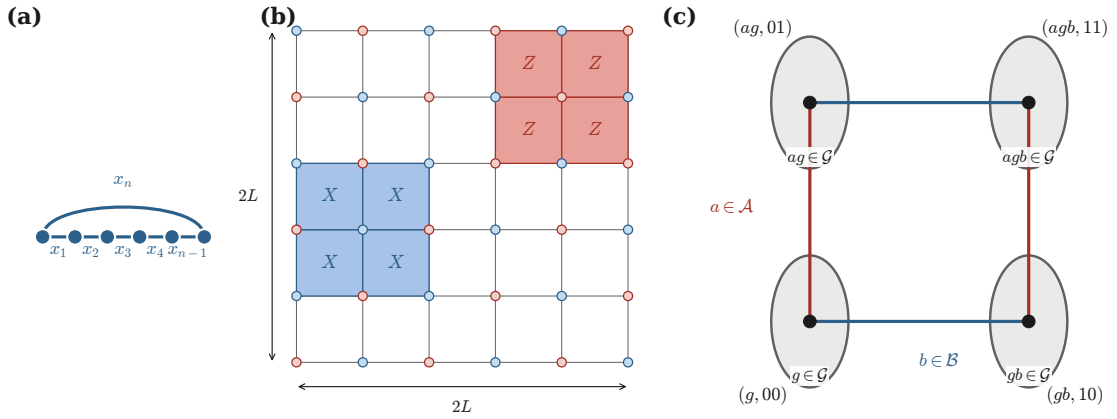


Figure 3: From the toric code to quantum Tanner codes. (a) Repetition code on a cycle. (b) The product of two cycles gives a 2D grid; qubits on squares and product-code constraints on vertices yield the rotated toric code $[[4L^2, 2, 2L]]$. (c) The LRCC built from a group $\mathcal{G}$ and multisets $\mathcal{A}, \mathcal{B}$ replaces the grid. Each vertex sees a $\Delta \times \Delta$ array of squares, and X/Z generators are codewords of $C_{\mathcal{A}} \otimes C_{\mathcal{B}}$ and $C_{\mathcal{A}}^{\perp} \otimes C_{\mathcal{B}}^{\perp}$. Figure from Ref. [2].

5 Outlook: Open Directions for Neutral-Atom Fault Tolerance

- **Hardware-aware syndrome extraction.** In Ref. [28] we compiled syndrome extraction for CSS codes onto two parallel arrays of shuttled spin qubits. For column-regular qLDPC codes with Shor-style extraction, the minimal number of shuttles equals the column weight; minimizing it for general codes is NP-hard. The product and group-action structure of MM and QT codes could likewise map onto AOD row–column moves of neutral atoms [6], with CNOT schedules (as with the left–right circuits above) chosen to keep circuit distance close to code distance.
- **Fewer syndrome rounds.** In our experiments MM codes reach low logical error rates with small decoding windows. On platforms where measurement and reset dominate the cycle time, fewer rounds per logical cycle translates directly into faster logical clocks.
- **Decoders and weight reduction.** Structure-aware decoders (cf. the `Frontier` result) and weight-reduction techniques that preserve fault distance [29] would make high-rate, high-weight instances practical.

References

[1] Feroz Ahmed Mian, Owen Gwilliam, and Stefan Krastanov. Multivariate multicycle codes for complete single-shot decoding. *arXiv preprint arXiv:2601.18879*, 2026. URL https://arxiv.org/abs/2601.18879.

[2] Feroz Ahmed Mian, Vaishnavi L. Addala, Arman Meraj, Adhiraj Chadha, and Stefan Krastanov. Quantum tanner codes at moderate blocklength. *arXiv preprint arXiv:2608.12509*, 2026. URL https://arxiv.org/abs/2608.12509.

[3] Anthony Leverrier, Wouter Rozendaal, and Gilles Zémor. Small quantum tanner codes from left–right cayley complexes. *arXiv preprint arXiv:2512.20532*, 2025.

[4] Sergey Bravyi, David Poulin, and Barbara Terhal. Tradeoffs for reliable quantum information storage in 2d systems. *Phys. Rev. Lett.*, 104:050503, Feb 2010. doi: 10.1103/PhysRevLett.104.050503. URL https://link.aps.org/doi/10.1103/PhysRevLett.104.050503.

[5] Sergey Bravyi, Andrew W. Cross, Jay M. Gambetta, Dmitri Maslov, Patrick Rall, and Theodore J. Yoder. High-threshold and low-overhead fault-tolerant quantum memory. *Nature*, 627(8005):778–782, March 2024. ISSN 1476-4687. doi: 10.1038/s41586-024-07107-7. URL http://dx.doi.org/10.1038/s41586-024-07107-7.

[6] Qian Xu, J Pablo Bonilla Ataides, Christopher A Pattison, Nithin Raveendran, Dolev Bluvstein, Jonathan Wurtz, Bane Vasić, Mikhail D Lukin, Liang Jiang, and Hengyun Zhou. Constant-overhead fault-tolerant quantum computation with reconfigurable atom arrays. *Nature Physics*, 20(7):1084–1090, 2024.

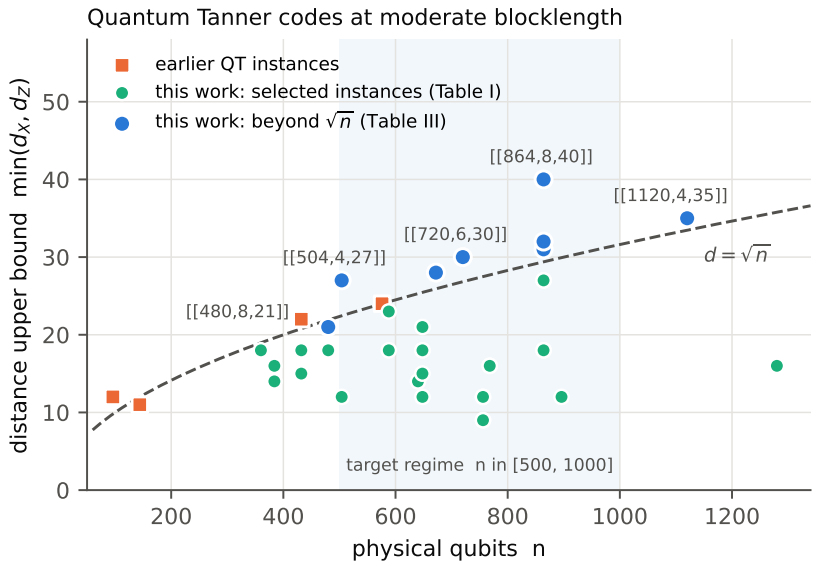


Figure 4: Distance upper bounds $\min(d_X, d_Z)$ versus blocklength for QT instances from Ref. [2], compared with earlier explicit instances [3, 23] and the $\sqrt{n}$ reference. Plotted from the tables of Ref. [2].

[7] Héctor Bombín. Single-shot fault-tolerant quantum error correction. *Physical Review X*, 5(3):031043, 2015.

[8] Earl T Campbell. A theory of single-shot error correction for adversarial noise. *Quantum Science and Technology*, 4(2):025006, February 2019. ISSN 2058-9565. doi: 10.1088/2058-9565/aafc8f. URL http://dx.doi.org/10.1088/2058-9565/aafc8f.

[9] Armanda O. Quintavalle, Michael Vasmer, Joschka Roffe, and Earl T. Campbell. Single-shot error correction of three-dimensional homological product codes. *PRX Quantum*, 2(2), June 2021. ISSN 2691-3399. doi: 10.1103/prxquantum.2.020340. URL http://dx.doi.org/10.1103/PRXQuantum.2.020340.

[10] Hsiang-Ku Lin, Pak Kau Lim, Alexey A. Kovalev, and Leonid P. Pryadko. Abelian multi-cycle codes for single-shot error correction, 2025. URL https://arxiv.org/abs/2506.16910.

[11] Eric Dennis, Alexei Kitaev, Andrew Landahl, and John Preskill. Topological quantum memory. *Journal of Mathematical Physics*, 43(9):4452–4505, September 2002. ISSN 1089-7658. doi: 10.1063/1.1499754. URL http://dx.doi.org/10.1063/1.1499754.

[12] Abraham Jacob, Campbell McLauchlan, and Dan E. Browne. Single-shot decoding and fault-tolerant gates with trivariate tricycle codes, 2025. URL https://arxiv.org/abs/2508.08191.

[13] L. P. Pryadko and W. Zeng. dist-m4ri— distance of a classical or quantum CSS code. https://github.com/QEC-pages/dist-m4ri, 2024. Accessed: 2026.

[14] Craig Gidney. Stim: a fast stabilizer circuit simulator. *Quantum*, 5:497, July 2021. ISSN 2521-327X. doi: 10.22331/q-2021-07-06-497. URL https://doi.org/10.22331/q-2021-07-06-497.

[15] Laleh Aghababaie Beni, Oscar Higgott, and Noah Shutty. Tesseract: A search-based decoder for quantum error correction, 2025. URL https://arxiv.org/abs/2503.10988.

[16] Joschka Roffe, David R. White, Simon Burton, and Earl Campbell. Decoding across the quantum low-density parity-check code landscape. *Physical Review Research*, 2(4), Dec 2020. ISSN 2643-1564. doi: 10.1103/physrevresearch.2.043423. URL http://dx.doi.org/10.1103/PhysRevResearch.2.043423.

[17] Luka Skoric, Dan E Browne, Kenton M Barnes, Neil I Gillespie, and Earl T Campbell. Parallel window decoding enables scalable fault tolerant quantum computation. *Nature Communications*, 14(1):7040, 2023.

[18] Armands Strikis, Dan E Browne, and Michael E Beverland. High-performance syndrome extraction circuits for quantum codes. *arXiv preprint arXiv:2603.05481*, 2026.

[19] Anthony Leverrier and Gilles Zémor. Quantum tanner codes. In *2022 IEEE 63rd Annual Symposium on Foundations of Computer Science (FOCS)*, pages 872–883, 2022. doi: 10.1109/FOCS54457.2022.00117.

[20] Hans Ulrich Besche, Bettina Eick, Eamonn O'Brien, and Max Horn. SmallGrp – The GAP Small Groups Library, Version 1.5.4, July 2024. URL https://gap-packages.github.io/smallgrp/. GAP package.

[21] Leonid P Pryadko, Vadim A Shabashov, and Valerii K Kozin. Qdistrnd: A gap package for computing the distance

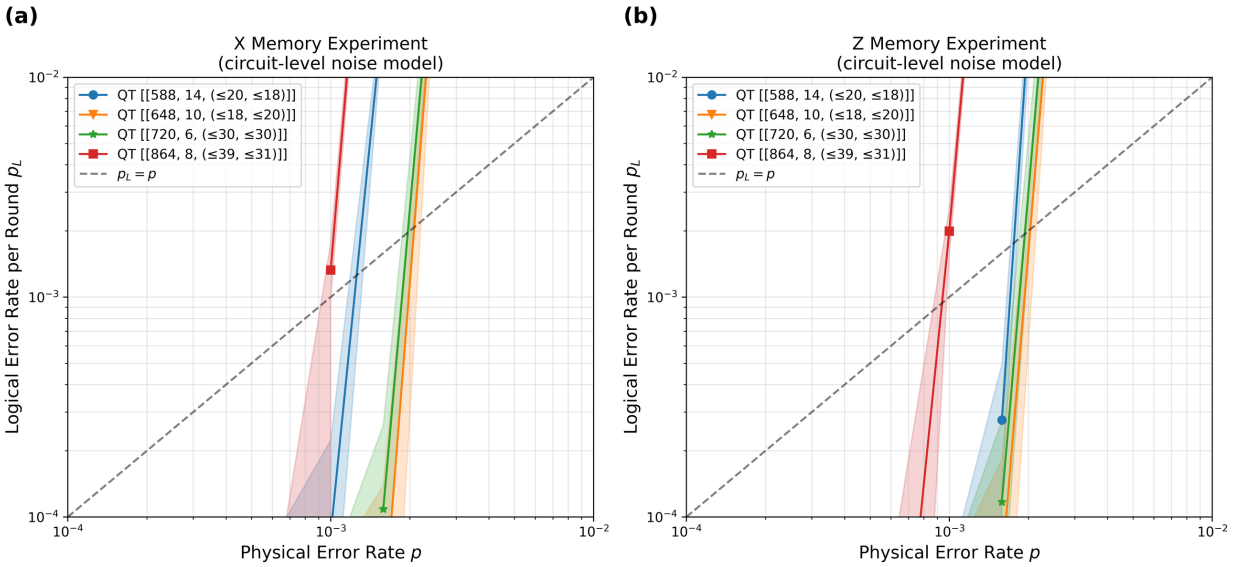


Figure 5: Per-round logical error rate versus physical error rate under circuit-level noise for (a) X and (b) Z memory experiments on four QT codes from our search, decoded with Tesseract. The dashed line marks $p_L = p$. Figure from Ref. [2].

of quantum error-correcting codes. *arXiv preprint arXiv:2308.15140*, 2023.

[22] Aditya Bhardwaj, Muzhou Ma, Nadine Meister, Robbie King, Dolev Bluvstein, John Preskill, Madelyn Cain, Qian Xu, and Hsin-Yuan Huang. High-rate qldpc processors. *arXiv preprint arXiv:2607.28795*, 2026.

[23] Virgile Guemard and Gilles Zémor. Moderate-length lifted quantum tanner codes. *arXiv preprint arXiv:2502.20297*, 2025.

[24] Anthony Leverrier and Rüdiger Urbanke. Approximating optimal decoding of quantum ldpc codes with narrow frontiers. *arXiv preprint arXiv:2606.20513*, 2026.

[25] QuantumClifford Contributors. QuantumSavory/QuantumClifford.jl: v0.10.1, September 2025. URL https://doi.org/10.5281/zenodo.13950271.

[26] OSCAR. OSCAR – Open Source Computer Algebra Research system, Version 1.5.0, 2025. URL https://www.oscar-system.org.

[27] JP Tillich and G Zémor. Quantum ldpc codes with positive rate and minimum distance proportional to n1/2, information theory, 2009. isit 2009.

[28] Anthony Micciche, Feroz Ahmed Mian, Anasua Chatterjee, Andrew McGregor, and Stefan Krastanov. Optimizing compilation of error correction codes for $2 \times n$ quantum dot arrays and its NP hardness. *Physical Review Research*, 8:013212, 2026. doi: 10.1103/l5y5-v3k7.

[29] Shi Jie Samuel Tan and Lev Stambler. Effective distance of higher dimensional hgps and weight-reduced quantum ldpc codes. *Quantum*, 9:1897, October 2025. ISSN 2521-327X. doi: 10.22331/q-2025-10-28-1897. URL http://dx.doi.org/10.22331/q-2025-10-28-1897.